International Journal of Heat and Mass Transfer 171 (2021) 121067

Contents lists available at ScienceDirect

International Journal of Heat and Mass Transfer

journal homepage: www.elsevier.com/locate/hmt

Technical Note

Heat transfer from a particle in laminar flows of a variable thermal conductivity fluid

Esmaeil Dehdashti[a], Meghdad Razizadeh[b], Hassan Masoud[a,*]

[a] Department of Mechanical Engineering-Engineering Mechanics, Michigan Technological University, Houghton, Michigan 49931, USA
[b] Department of Mechanical Engineering and Mechanics, Lehigh University, Bethlehem, PA 18015, USA

ARTICLE INFO

Article history:
Received 27 November 2020
Revised 13 January 2021
Accepted 5 February 2021

Keywords:
Convection heat transfer
Variable thermal conductivity
Laminar flow

ABSTRACT

We revisit the classical problem of steady-state heat transfer from a single particle in a uniform laminar flow with the assumption that the thermal conductivity of the fluid changes linearly with the temperature. We use a combination of asymptotic and scaling analyses to derive approximate expressions for the dimensionless heat transfer coefficient, i.e., the Nusselt number Nu, of arbitrarily shaped particles. The results cover the entire range of the Peclet number Pe. We find that, for a constant temperature boundary condition and fixed geometry, the Nusselt number is essentially equal to the product of two terms, one of which is only a function of Pe while the other one is nearly independent of Pe and mainly depends on the proportionality constant of the conductivity-temperature relation. We also show that, in contrast, when a uniform heat flux is imposed on the surface of the particle, Nu can be estimated as a summation of a Pe-dependent piece and one that solely varies with the proportionality constant.

1. Introduction

Heat transfer from a hot or cold object exposed to an external fluid flow is arguably the most basic form of forced convection heat transfer encountered in industrial processes and technological applications. When analyzing this category of heat transfer problems, in many cases, it is well justified to assume that the fluid properties such as density ρ, viscosity μ, specific heat c_p, and thermal conductivity k are constant. In general, this assumption renders the energy equation (the partial differential equation that governs the distribution of the fluid temperature) linear and decoupled from the Navier-Stokes equations (from which the fluid velocity field is determined).

There exist, however, practical cases where at least one of the fluid properties cannot realistically be considered constant. For instance, it has been shown that the effective thermal conductivity of nanofluids increases considerably with the rising temperature (see e.g., [1]) or, for liquid metals, k has been found to vary roughly linearly with the temperature in a wide range of operating conditions (see, e.g., [2]). The energy equation in these situations is no longer linear and, therefore, becomes more challenging to solve, which is the cost of adding realism to the mathematical model of the underlying transport phenomenon. Perhaps for this reason, the majority of textbook examples and classical problems in convective heat transfer from objects are solved under the assumption that the fluid properties are constant. Hence, it is of both academic and practical interest to revisit those problems with the goal of extending their solutions to cases with variable fluid properties. To this end, here, we examine the steady-state transfer of heat from a particle via an externally driven laminar flow, with the premise that the thermal conductivity of the fluid is a linear function of the temperature.

Building on previous theoretical efforts on the subject (see, e.g., [3–16]), we derive approximate expressions for the Nusselt number of particles of arbitrary geometry. The derivations are based on asymptotic and scaling analyses. For completeness, we consider both constant temperature and uniform heat flux boundary conditions on the surface of the particle. The results are presented for the full range of Peclet number Pe. In what follows, we first describe the problem we wish to solve (Section 2). Then, we present the solutions for the above-mentioned surface conditions (Section 3 and Section 4). The validity ranges of the solutions are discussed next (Section 5) and a brief summary is given in the end (Section 6).

2. Problem statement

Consider a laminar, steady-state, incompressible flow with velocity $\boldsymbol{u}$ past a stationary object of arbitrary geometry and characteristic length ℓ. Suppose that the free-stream velocity takes the

* Corresponding author.
E-mail address: hmasoud@mtu.edu (H. Masoud).

https://doi.org/10.1016/j.ijheatmasstransfer.2021.121067
0017-9310/

form of $\boldsymbol{U}_\infty = U_\infty \boldsymbol{e}$, where $U_\infty = |\boldsymbol{U}_\infty|$ is a constant and $\boldsymbol{e}$ is a unit vector, and that the temperature approaches a constant value, denoted $T^\star_\infty$, at large distances from the particle. Also, let the thermal conductivity of the fluid vary with the dimensionless temperature as $k = k_0(1+\beta T)$, with k_0 and β being the far-field conductivity and a constant parameter, respectively. Then, neglecting viscous dissipation, the equation that governs the steady-state distribution of T outside the particle is

$$\mathrm{Pe}\, \boldsymbol{u} \cdot \nabla T = \nabla \cdot [(1+\beta T)\nabla T], \tag{1}$$

where the Peclet number is defined as $\mathrm{Pe} = \rho U_\infty c_p \ell / k_0$. The boundary conditions associated with Eq. (1) are

$$T = 1 \quad \text{for} \quad \mathbf{r} \in S_p \quad \text{and} \quad \lim_{r\to\infty} T = 0 \tag{2}$$

for the case in which the surface of the particle S_p is held at a constant temperature T_s, and

$$(1+\beta T)\big(\mathbf{n} \cdot \nabla T\big) = -1 \quad \text{for} \quad \mathbf{r} \in S_p \quad \text{and} \quad \lim_{r\to\infty} T = 0 \tag{3}$$

for the one where a uniform heat flux q_s is applied on S_p. Here, $\boldsymbol{r}$ is the position vector with magnitude $r = |\boldsymbol{r}|$ and $\boldsymbol{n}$ is the unit vector outward normal to the surface of the particle. Furthermore, the length and fluid velocity are non-dimensionalized, respectively, by ℓ and U_∞, whereas the dimensionless temperature is defined as either

$$\frac{T^\star - T^\star_\infty}{T^\star_s - T^\star_\infty} \quad \text{or} \quad \frac{T^\star - T^\star_\infty}{q_s\, \ell / k_0}, \tag{4}$$

consistent with the boundary conditions in Eqs. (2) and (3). The star superscript is used to denote the dimensional temperature.

A key dimensionless quantity in analyzing the boundary-value problems described by Eqs. (1)–(3) is the average Nusselt number, which can be defined as

$$\mathrm{Nu}_{T} = -\frac{1+\beta}{2\pi} \int_{S_p} \mathbf{n} \cdot \nabla T \, \mathrm{d}S \tag{5}$$

for the problem with a prescribed temperature on the surface of the particle (see Eq. (2)) and as

$$\mathrm{Nu}_{Q} = \frac{\mathbb{S}_p}{2\pi\, \overline{T}} \tag{6}$$

for the one with a prescribed heat flux on S_p (see Eq. (3)), where $\mathbb{S}_p$ represents the dimensionless surface area of the particle and $\overline{T}$ is the mean value of T on S_p. In the following sections, we seek to develop approximate formulas for the variations of Nu_{T} and Nu_{Q} with Pe and β.

3. Variation of Nu_{T} as a function of Pe and β

We begin the derivation of Nu_{T} by first considering the asymptotic limits of small and large Peclet numbers and then bridging the gap between the two limits by introducing a smooth transition function. Our approach builds on ideas presented in the classical works on the topic of heat and mass transfer from an isolated particle in uniform flows (see, e.g., [5–7,17–19]).

3.1. Limit of conduction-dominated heat transport

Suppose conduction is the dominant mode of heat transport, i.e., $\mathrm{Pe} \ll 1$, but finite. In this limit, an effective approach for dealing with the nonlinearity of Eq. (1) is to make a change of variable from T to θ such that

$$\theta = \frac{1}{k_0}\int_0^T k(\mathcal{T})\,\mathrm{d}\mathcal{T} = \int_0^T (1+\beta\mathcal{T})\mathrm{d}\mathcal{T} = \frac{\beta}{2}T^2 + T. \tag{7}$$

This is known as the Kirchhoff transformation (see, e.g., [6,10]), with the reference temperature set to $T=0$ for convenience. It follows from Eq. (7) that

$$\mathrm{Nu}_{T} = -\frac{1}{2\pi}\int_{S_p} \mathbf{n} \cdot \nabla\theta \, \mathrm{d}S, \tag{8}$$

where

$$\begin{aligned} &Pe\, \mathbf{u} \cdot \frac{\nabla\theta}{\sqrt{1+2\beta\theta}} = \nabla^2\theta, \quad \text{with} \\ &\theta = 1+\beta/2 \quad \text{for} \quad \mathbf{r}\in S_p \quad \text{and} \quad \lim_{r\to\infty}\theta = 0. \end{aligned} \tag{9}$$

Our goal is to obtain an asymptotic expression for Nu_{T}, and, to that end, we proceed with a singular perturbation expansion of θ in terms of Pe (see, e.g, [6,17,20]). In particular, we assume that, in the vicinity of the particle, θ can be expressed as

$$\theta = \theta^{(0)} + \mathrm{Pe}\,\theta^{(1)} + o(\mathrm{Pe}), \tag{10}$$

which is known as the inner expansion of θ. Upon substitution of Eq. (10) into Eqs. (8) and (9), we obtain

$$\begin{aligned} \mathrm{Nu}_T &= \mathrm{Nu}^{(0)}_{T} + \mathrm{Pe}\,\mathrm{Nu}^{(1)}_{T} + o(\mathrm{Pe}) \\ &= -\frac{1}{2\pi}\left[\int_{S_p} \mathbf{n}\cdot\nabla\theta^{(0)}\,\mathrm{d}S + \mathrm{Pe}\int_{S_p}\mathbf{n}\cdot\nabla\theta^{(1)}\,\mathrm{d}S\right] + o(\mathrm{Pe}), \end{aligned} \tag{11}$$

$$\nabla^2\theta^{(0)} = 0 \quad \text{with} \quad \theta^{(0)} = 1+\beta/2 \quad \text{for} \quad \mathbf{r}\in S_p. \tag{12}$$

Far from the particle, on the other hand, we consider θ to take the form of

$$\tilde{\theta} = \mathrm{Pe}\,\tilde{\theta}^{(1)} + o(\mathrm{Pe}). \tag{13}$$

This is called the outer expansion of θ, where the tilde overbar denotes that the transformed temperature field is written as a function of the rescaled position vector

$$\tilde{\boldsymbol{r}} = \mathrm{Pe}\,\boldsymbol{r} \quad \text{with} \quad \tilde{r} = |\tilde{\boldsymbol{r}}|. \tag{14}$$

Rewriting Eq. (9) in terms of $\tilde{\boldsymbol{r}}$ and replacing Eq. (13) for $\tilde{\theta}$, we find

$$\boldsymbol{e}\cdot\tilde{\nabla}\tilde{\theta}^{(1)} = \tilde{\nabla}^2\tilde{\theta}^{(1)} \quad \text{with} \quad \lim_{\tilde{r}\to\infty}\tilde{\theta}^{(1)} = 0, \tag{15}$$

with $\tilde{\nabla}$ and $\tilde{\nabla}^2$ operators representing derivatives with respect to the stretched coordinates. The inner and outer expansions are required to match asymptotically, i.e.,

$$\lim_{r\to\infty}\theta = \lim_{\tilde{r}\to 0}\tilde{\theta}. \tag{16}$$

Enforcing the above equation at every order of Pe furnishes the missing boundary conditions of Eqs. (12) and (15). Following Brenner [17], the zeroth-order inner solution away from the particle and the first-order outer solution can be written, respectively, as

$$\theta^{(0)} = \frac{\mathrm{Nu}^{(0)}_{T}}{2r} + O(r^{-3}) = \mathrm{Pe}\,\frac{\mathrm{Nu}^{(0)}_{T}}{2\tilde{r}} + O(\mathrm{Pe}^{-3}), \tag{17}$$

$$\tilde{\theta}^{(1)} = \frac{\mathrm{Nu}^{(0)}_{T}}{2\tilde{r}}\exp\left[-\frac{1}{2}(\tilde{r} - \boldsymbol{e}\cdot\tilde{\boldsymbol{r}})\right], \tag{18}$$

where $\boldsymbol{r}$ is measured from a proper origin located at the particle's "heat center".

Now, we take a shortcut approach that allows us to calculate $\mathrm{Nu}^{(1)}_{T}$ without directly solving for $\theta^{(1)}$. The technique is based on Greens second identity and falls under the general framework of the reciprocal theorem (see, e.g., [20–23]). First, we multiply Eq. (12) by θ and Eq. (9) by $\theta^{(0)}$. Next, we subtract the resulting equations and make some rearrangements to arrive at

$$\nabla\cdot\left(\theta\,\nabla\theta^{(0)}\right) = \nabla\cdot\left(\theta^{(0)}\,\nabla\theta\right) - \mathrm{Pe}\,\boldsymbol{u}\cdot\frac{\theta^{(0)}\,\nabla\theta}{\sqrt{1+2\beta\theta}}. \tag{19}$$

Then, we integrate Eq. (19) over the fluid domain V and use the divergence theorem to reach

$$\int_{S_p} \theta\, \boldsymbol{n} \cdot \nabla\theta^{(0)}\, \mathrm{d}S = \int_{S_p} \theta^{(0)} \boldsymbol{n} \cdot \nabla\theta\, \mathrm{d}S + \mathrm{Pe} \int_V \boldsymbol{u} \cdot \frac{\theta^{(0)}\, \nabla\theta}{\sqrt{1+2\beta\theta}}\, \mathrm{d}V. \tag{20}$$

Note that the contributions from surfaces at infinity (denoted by S_∞) vanish because the integrands decay faster than dS grows at large distances from the particle. Eq. (20) can be simplified to

$$\mathrm{Nu}_T = \mathrm{Nu}_T^{(0)} + \frac{\mathrm{Pe}}{2\pi(1+\beta/2)} \int_V \boldsymbol{u} \cdot \frac{\theta^{(0)}\, \nabla\theta}{\sqrt{1+2\beta\theta}}\, \mathrm{d}V \tag{21}$$

by applying the boundary conditions on S_p.

Inspecting Eqs. (21), (13), (11), and (10), we determine that

$$\mathrm{Nu}_T^{(1)} = \frac{1}{2\pi(1+\beta/2)} \times \left[\int_V \boldsymbol{u} \cdot \frac{\theta^{(0)}\, \nabla\theta^{(0)}}{\sqrt{1+2\beta\theta^{(0)}}}\, \mathrm{d}V + \boldsymbol{e} \cdot \int_{\mathbb{R}^3} \tilde{\theta}^{(0)}\, \tilde{\nabla}\left(\tilde{\theta}^{(1)} - \tilde{\theta}^{(0)}\right) \mathrm{d}\tilde{\boldsymbol{r}} \right], \tag{22}$$

where the second integral on the right-hand side is over the entire three-dimensional real space $\mathbb{R}^3$ and $\tilde{\theta}^{(0)} = \mathrm{Nu}_T^{(0)}/2\tilde{r}$. We proceed with evaluating the integral appearing first on the right-hand side of Eq. (22). To that effect, we convert this volume integral into a pair of surface integrals as

$$\begin{aligned} &\int_V \mathbf{u} \cdot \frac{\theta^{(0)}\, \nabla\theta^{(0)}}{\sqrt{1+2\beta\theta^{(0)}}}\, \mathrm{d}V \\ &= \frac{1}{3\beta^2} \int_V \nabla \cdot \left[\sqrt{1+2\beta\theta^{(0)}} \left(\beta\theta^{(0)} - 1\right) \mathbf{u} \right] \mathrm{d}V \\ &= -\frac{1}{3\beta^2} \left[\int_{S_p} \sqrt{1+2\beta\theta^{(0)}} \left(\beta\theta^{(0)} - 1\right) \mathbf{n} \cdot \mathbf{u}\, \mathrm{d}S \right. \\ &\qquad \left. + \int_{S_\infty} \sqrt{1+2\beta\theta^{(0)}} \left(\beta\theta^{(0)} - 1\right) \mathbf{n} \cdot \mathbf{u}\, \mathrm{d}S \right]. \end{aligned} \tag{23}$$

Due to no penetration condition, $\boldsymbol{n} \cdot \boldsymbol{u} = 0$ on S_p. Also,

$$\int_{S_\infty} \boldsymbol{n} \cdot \boldsymbol{u}\, \mathrm{d}S = 0 \tag{24}$$

because the flow is incompressible (i.e, $\nabla \cdot \boldsymbol{u} = 0$). Therefore, the values of both surface integrals in Eq. (23) amount to zero, which means that the volume integral is zero, too. Additionally,

$$\begin{aligned} &\boldsymbol{e} \cdot \int_{\mathbb{R}^3} \tilde{\theta}^{(0)}\, \tilde{\nabla}\tilde{\theta}^{(0)}\, \mathrm{d}\tilde{\boldsymbol{r}} \\ &= -\frac{\left(\mathrm{Nu}_T^{(0)}\right)^2}{4} \int_0^\infty \frac{1}{\tilde{r}} \int_0^\pi \sin^2\theta \int_0^{2\pi} \cos\varphi\, \mathrm{d}\varphi\, \mathrm{d}\theta\, \mathrm{d}\tilde{r} = 0. \end{aligned} \tag{25}$$

Incorporating these results, we find (after algebraic manipulations) that

$$\begin{aligned} \mathrm{Nu}_T^{(1)} &= \frac{\left(\mathrm{Nu}_T^{(0)}\right)^2}{8\pi(1+\beta/2)} \int_{\mathbb{R}^3} \frac{\boldsymbol{e} \cdot \tilde{\boldsymbol{r}}}{\tilde{r}^4} \exp\left[-\frac{1}{2}(\tilde{r} - \boldsymbol{e} \cdot \tilde{\boldsymbol{r}})\right] \mathrm{d}\tilde{\boldsymbol{r}} \\ &= \frac{\left(\mathrm{Nu}_T^{(0)}\right)^2}{4(1+\beta/2)}. \end{aligned} \tag{26}$$

The evaluation of the volume integral over $\mathbb{R}^3$ is detailed by Dehdashti and Masoud [20].

Replacing for $\mathrm{Nu}_T^{(1)}$ in Eq. (11), we have

$$\begin{aligned} \mathrm{Nu}_T &= (1+\beta/2) \left[\frac{\mathrm{Nu}_T^{(0)}}{1+\beta/2} + \frac{\mathrm{Pe}}{4} \left(\frac{\mathrm{Nu}_T^{(0)}}{1+\beta/2} \right)^2 + o(\mathrm{Pe}) \right] \\ &= (1+\beta/2) \left[\mathrm{Nu}_{T,0}^{(0)} + \mathrm{Pe}\, \frac{\left(\mathrm{Nu}_{T,0}^{(0)}\right)^2}{4} + o(\mathrm{Pe}) \right] \\ &= (1+\beta/2)\mathrm{Nu}_{T,0} + o(\mathrm{Pe}), \end{aligned} \tag{27}$$

where $\mathrm{Nu}_{T,0}$ and $\mathrm{Nu}_{T,0}^{(0)}$ are the Nusselt numbers corresponding, respectively, to $\beta = 0$ and to $\beta = 0$ and $\mathrm{Pe} = 0$. In other words, the former is the constant conductivity Nusselt number and the latter is the constant conductivity pure conduction Nusselt number. Remember that Eq. (12) describes a linear boundary value problem and, therefore, changing its boundary condition on S_p from $\theta = 1+\beta/2$ to $\theta = 1$ alters the respective Nusselt number by a factor of $(1+\beta/2)^{-1}$.

Eq. (27) indicates that, to the leading order in Pe, Nu_T is the product of a β-dependent term and the constant-conductivity Nusselt number, which depends on Pe and the geometry of the particle. It is worth emphasizing that this relation was derived with no restriction on the flow Reynolds number, defined as $\mathrm{Re} = \rho U_\infty \ell/\mu$. Even no-slip condition was not necessary. The only conditions enforced were the flow incompressibility and no flow penetration into the particle. Lastly, we note that Eq. (27) recovers the classical result of Brenner [17] for $\beta = 0$ and generalizes the work of Polyanin [6] for the special case of Stokes flow (i.e., $\mathrm{Re} = 0$).

3.2. Limit of advection-dominated heat transport

Suppose the transport of heat is dominated by advection, i.e., $\mathrm{Pe} \gg 1$. In this limit, the temperature outside the particle approaches T_∞ at short distances from S_p. In other words, the temperature variations are confined to a narrow layer next to the boundary of the particle. Here, similar to Section 3.1, we aim for developing an asymptotic approximation for the Nusselt number.

Assuming that S_p is smooth, we follow Polyanin [5] and adopt a *generalized* boundary layer coordinate system $(\mathrm{x}, \mathrm{y}, \mathrm{z})$, with the corresponding unit vectors $\boldsymbol{e}_\mathrm{x}$, $\boldsymbol{e}_\mathrm{y}$, and $\boldsymbol{e}_\mathrm{z}$, and associated metric coefficients h_x, h_y, and h_z. Remember that, throughout the paper, all lengths are non-dimensionalized by ℓ. The y component in this system measures the distance from the surface of the particle and, thus, $\boldsymbol{e}_\mathrm{y} = \boldsymbol{n}$ at $\mathrm{y} = 0$ (i.e., at S_p). The direction of the x coordinate is chosen to be the same as the component of the fluid velocity vector projected onto the plane normal to $\boldsymbol{e}_\mathrm{y}$. The direction of the third coordinate is then determined by $\boldsymbol{e}_\mathrm{z} = \boldsymbol{e}_\mathrm{x} \times \boldsymbol{e}_\mathrm{y}$.

Eq. (1), written in terms of the $(\mathrm{x}, \mathrm{y}, \mathrm{z})$ coordinates, takes the form of

$$\begin{aligned} &\mathrm{Pe}\left(\frac{u_\mathrm{x}}{h_\mathrm{x}} \frac{\partial T}{\partial \mathrm{x}} + \frac{u_\mathrm{y}}{h_\mathrm{y}} \frac{\partial T}{\partial \mathrm{y}} \right) = \frac{1}{h_\mathrm{x} h_\mathrm{y} h_\mathrm{z}} \left\{ \frac{\partial}{\partial \mathrm{x}} \left[\frac{h_\mathrm{y} h_\mathrm{z}}{h_\mathrm{x}} \frac{\partial}{\partial \mathrm{x}} \left(T + \frac{\beta}{2} T^2 \right) \right] \right. \\ &\left. + \frac{\partial}{\partial \mathrm{y}} \left[\frac{h_\mathrm{x} h_\mathrm{z}}{h_\mathrm{y}} \frac{\partial}{\partial \mathrm{y}} \left(T + \frac{\beta}{2} T^2 \right) \right] + \frac{\partial}{\partial \mathrm{z}} \left[\frac{h_\mathrm{x} h_\mathrm{y}}{h_\mathrm{z}} \frac{\partial}{\partial \mathrm{z}} \left(T + \frac{\beta}{2} T^2 \right) \right] \right\} \\ &\text{with} \quad T = 1 \quad \text{at} \quad \mathrm{y} = 0 \quad \text{and} \quad \lim_{\mathrm{y} \to \infty} T = 0. \end{aligned} \tag{28}$$

In the above equation,

$$u_\mathrm{x} = \frac{1}{h_\mathrm{y} h_\mathrm{z}} \frac{\partial \Psi}{\partial \mathrm{y}} \quad \text{and} \quad u_\mathrm{y} = -\frac{1}{h_\mathrm{x} h_\mathrm{z}} \frac{\partial \Psi}{\partial \mathrm{x}} \tag{29}$$

are the velocity components in the x and y directions, respectively, where Ψ is a pseudo stream function. Note that u_z is zero per the definition of the generalized boundary layer coordinate system. Given that the distribution of temperature is restricted to a thin region close to S_p, it is convenient to expand the metric coefficients and Ψ about $\mathrm{y} = 0$ as

$$h_\mathrm{x} = h_{\mathrm{x},0}(\mathrm{x}, \mathrm{z}) + h_{\mathrm{x},1}(\mathrm{x}, \mathrm{z})\, \mathrm{y} + \cdots, \tag{30}$$

$$h_\mathrm{y} = 1, \tag{31}$$

$$h_\mathrm{z} = h_{\mathrm{z},0}(\mathrm{x}, \mathrm{z}) + h_{\mathrm{z},1}(\mathrm{x}, \mathrm{z})\, \mathrm{y} + \cdots, \tag{32}$$

$$\Psi = \frac{1}{2}\Psi_2(x, z)\, y^2 + \cdots, \tag{33}$$

where

$$\Psi_2 = \left(h_z \frac{\partial u_x}{\partial y} \right)_{y=0} = h_{z,0}\, \tau_0, \tag{34}$$

with τ_0 being the dimensionless shear stress at the surface of the particle. To ensure the validity of Eq. (33), the Prandtl number $\mathrm{Pr} = c_p \mu / k_0$ is assumed to be large. Needless to say, both Ψ and $\partial\Psi/\partial y$ are zero at $y = 0$, due to the no-slip condition.

The thickness of the temperature boundary layer is known to scale with $\mathrm{Pe}^{-1/3}$, which results from equating the order of magnitude of the advective and conductive terms within the boundary layer (see, e.g., [18,19]). Considering this scaling and the structure of Eq. (28), we proceed with expanding T and Nu_T as

$$T = T^{(0)}(x, \tilde{y}, z) + O(\mathrm{Pe}^{-1/3}), \tag{35}$$

$$\mathrm{Nu}_T = \mathrm{Pe}^{1/3}\, \mathrm{Nu}_T^{(0)} + O(1) \tag{36}$$

and with making the following change of variables:

$$Y = \mathrm{Pe}^{1/3}\, y, \tag{37}$$

$$X = \int_{x_0}^{x} h_{x,0}\, h_{z,0}\, d\hat{x}. \tag{38}$$

Next, we rewrite Eq. (28) to the leading order in Pe as

$$Y\,\Psi_2 \frac{\partial T^{(0)}}{\partial X} - \frac{Y^2}{2}\frac{\partial \Psi_2}{\partial X}\frac{\partial T^{(0)}}{\partial Y} = \frac{\partial^2}{\partial Y^2}\left[T^{(0)} + \frac{\beta}{2}\left(T^{(0)}\right)^2 \right]$$

$$\text{with} \quad T^{(0)} = 1 \quad \text{at} \quad Y = 0 \quad \text{and} \quad \lim_{Y\to\infty} T^{(0)} = 0. \tag{39}$$

Eq. (39) can be further simplified to its self-similar form

$$\frac{d^2}{d\eta^2}\left[T^{(0)} + \frac{\beta}{2}\left(T^{(0)}\right)^2 \right] + 3\,\eta^2 \frac{dT^{(0)}}{d\eta} = 0 \quad \text{with}$$

$$T^{(0)} = 1 \quad \text{at} \quad \eta = 0 \quad \text{and} \quad \lim_{\eta\to\infty} T^{(0)} = 0, \tag{40}$$

where the new independent variable η is defined, according to the von Mises transformation, via

$$\eta = \sqrt{\Psi_2}\left(9 \int_{X_0}^{X} \sqrt{\Psi_2}\, d\hat{X} \right)^{-1/3} Y. \tag{41}$$

Taking everything into account, the leading-order term in the Nusselt number expansion can be expressed as

$$\begin{aligned} \mathrm{Nu}_T^{(0)} &= -\left(\frac{1+\beta}{2\pi}\right) \int_{S_p} \left.\frac{\partial T^{(0)}}{\partial \tilde{y}}\right|_{\tilde{y}=0} dS \\ &= -\left(\frac{1+\beta}{4\pi}\right) \left.\frac{dT^{(0)}}{d\eta}\right|_{\eta=0} \int_{z_{\min}}^{z_{\max}} \left(\int_{X_{\min}}^{X_{\max}} \sqrt{3\,\Psi_2}\, dX \right)^{2/3} dz \\ &= (1+\beta) \left.\frac{dT^{(0)}}{d\eta}\right|_{\eta=0} \left(\left.\frac{dT^{(0)}}{d\eta}\right|_{\eta=0,\,\beta=0} \right)^{-1} \mathrm{Nu}_{T,0}^{(0)} \\ &= -\Gamma\left(\frac{4}{3}\right)(1+\beta) \left.\frac{dT^{(0)}}{d\eta}\right|_{\eta=0} \mathrm{Nu}_{T,0}^{(0)}, \end{aligned} \tag{42}$$

where $\mathrm{Nu}_{T,0}^{(0)}$ represents the value of $\mathrm{Nu}_T^{(0)}$ corresponding to $\beta = 0$. Of course, Eq. (42) reproduces the classical results of Lighthill [24] and Acrivos [25]. We demonstrate, in Appendix A, that the prefactor c is

$$c = -\Gamma\left(\frac{4}{3}\right)(1+\beta) \left.\frac{dT^{(0)}}{d\eta}\right|_{\eta=0} \approx \left(1 + \frac{3\beta}{5}\right)^{2/3}. \tag{43}$$

Hence, we obtain

$$\mathrm{Nu}_T \approx \left(1 + \frac{3\beta}{5}\right)^{2/3} \mathrm{Nu}_{T,0} + O(1), \tag{44}$$

with $\mathrm{Nu}_{T,0}$ denoting the Nusselt number for the case of $\beta = 0$.

3.3. Bridging results for limits of low and high Peclet numbers

The results of the previous two subsections can be described succinctly as

$$\left.\begin{aligned} \frac{\mathrm{Nu}_T}{\mathrm{Nu}_{T,0}} &\approx \left(1 + \frac{\beta}{2}\right) && \text{for} \quad \mathrm{Pe} \ll 1 \\ \frac{\mathrm{Nu}_T}{\mathrm{Nu}_{T,0}} &\approx \left(1 + \frac{3\beta}{5}\right)^{2/3} && \text{for} \quad \mathrm{Pe} \gg 1 \end{aligned}\right\} \Rightarrow \frac{\mathrm{Nu}_T}{\mathrm{Nu}_{T,0}} \approx (1 + a\,\beta)^b, \tag{45}$$

where $1/2 \lessapprox a \lessapprox 3/5$ and $2/3 \lessapprox b \lessapprox 1$. The functional dependency of these two parameters on the Peclet number may be formulated as

$$a \approx \frac{(3/5)\sqrt{\mathrm{Pe}} + a_0}{\sqrt{\mathrm{Pe}} + 2a_0}, \tag{46}$$

$$b \approx \frac{(2/3)\sqrt{\mathrm{Pe}} + b_0}{\sqrt{\mathrm{Pe}} + b_0}, \tag{47}$$

where

$$a_0 = 5.78 \quad \text{and} \quad b_0 = 5.90. \tag{48}$$

The above relations are motivated by the full numerical solution of Eq. (1), subject to the boundary conditions in Eq. (2), for several basic particle shapes. The accuracy of the predictions made by Eqs. (45)–(48) and the details of the numerical solutions will be discussed in Section 5. Note that, for some simple geometries, approximate formulas are available for $\mathrm{Nu}_{T,0}$ (see, e.g., [20] and references therein).

Overall, our asymptotic analyses in this section (summarized by Eq. (5)) suggest that the ratio between the Nusselt number and its corresponding value for the case of constant conductivity (i.e., $\beta = 0$) is approximately equal to a term that is mainly a function of β, while being weakly dependent on Pe. It is important to emphasize that this result was derived for particles of arbitrary shape under a fairly general flow condition, namely a laminar, steady-state, incompressible flow. We have only demanded the Prandtl number to be large when the Peclet number is high.

4. Variation of Nu_Q as a function of Pe and β

In Section 3, we considered Eq. (1) assuming that the surface of the particle is held at a constant temperature (see Eq. (2)). There, the assumption of a Dirichlet boundary condition on S_p allowed us to effectively employ the Kirchhoff and von Mises transformations (for, respectively, $\mathrm{Pe} \ll 1$ and $\mathrm{Pe} \gg 1$) to develop a nearly analytical formula for Nu_T. Unfortunately, neither techniques can be directly applied to find the general form of the Nusselt number when a uniform heat flux is imposed on S_p. That a Neumann boundary condition is more challenging to deal with analytically than its Dirichlet counterpart is a known matter (see, e.g., [20]). Despite this difficulty, we derive an estimate for Nu_Q with the aid of the following scaling arguments.

4.1. Limit of conduction-dominated heat transport

Consider the limit of $\mathrm{Pe} \ll 1$, and, accordingly, an inner expansion of the form

$$T = T^{(0)} + \mathrm{Pe}\, T^{(1)} + \cdots \tag{49}$$

for the temperature, where

$$\nabla\cdot\left[\left(1+\beta T^{(0)}\right)\nabla T^{(0)}\right]=0 \quad \text{with} \quad \left(1+\beta T^{(0)}\right)\left(\mathbf{n}\cdot\nabla T^{(0)}\right)=-1 \quad \text{for} \quad \mathbf{r}\in S_p \quad \text{and} \quad \lim_{r\to\infty} T^{(0)}=0 \tag{50}$$

and

$$\mathbf{n}\cdot\nabla T^{(0)}=\nabla^2\left(T^{(1)}+\beta T^{(0)}T^{(1)}\right) \quad \text{with} \quad \mathbf{n}\cdot\nabla\left(T^{(1)}+\beta T^{(0)}T^{(1)}\right)=0 \quad \text{for} \quad \mathbf{r}\in S_p. \tag{51}$$

Applying the Kirchhoff transformation (see Eq. (7)), it can be shown that

$$T^{(0)}=\frac{\sqrt{1+2\beta\theta^{(0)}}-1}{\beta}, \tag{52}$$

where

$$\begin{aligned}\nabla^2\theta^{(0)} &= 0 \quad \text{with}\\ \mathbf{n}\cdot\nabla\theta^{(0)} &= -1 \quad \text{for} \quad \mathbf{r}\in S_p \quad \text{and} \quad \lim_{r\to\infty}\theta^{(0)}=0.\end{aligned} \tag{53}$$

Additionally, consistent with Eq. (49), the Nusselt number can be expressed as

$$\begin{aligned}\mathrm{Nu}_{\mathrm{Q}} &= \frac{\mathbb{S}_p}{2\pi\overline{T}^{(0)}}\left(1-\mathrm{Pe}\,\frac{\overline{T}^{(1)}}{\overline{T}^{(0)}}\right)+\cdots\\ &= \mathrm{Nu}_{\mathrm{Q}}^{(0)}+\mathrm{Pe}\,\mathrm{Nu}_{\mathrm{Q}}^{(1)}+\cdots,\end{aligned} \tag{54}$$

where the overbar indicates average over S_p (see also Eq. (6)). The zeroth-order Nusselt number is determined by the solution of Eq. (53), with its dependency on β obeying Eq. (52). How about the dependency of $\mathrm{Nu}_{\mathrm{Q}}^{(1)}$ on β? To find this out, we examine the limits of small and large β.

Suppose $\beta \ll 1$, in which case we can write

$$\mathrm{Nu}_{\mathrm{Q}}^{(1)}=\mathrm{Nu}_{\mathrm{Q},0}^{(1)}+\beta\,\mathrm{Nu}_{\mathrm{Q},1}^{(1)}+\cdots. \tag{55}$$

Since both Pe and β are small, then, we need to only retain $\mathrm{Nu}_{\mathrm{Q},0}^{(1)}$ in the above expansion. This means that, to the leading order, $\mathrm{Nu}_{\mathrm{Q}}^{(1)}$ is independent of β. Now, assume $\beta \gg 1$. Eqs. (52) and (51) suggest that, in this limit,

$$T^{(0)}\sim\frac{1}{\sqrt{\beta}} \quad \text{and} \quad T^{(1)}\sim\frac{1}{\beta}. \tag{56}$$

Hence, we conclude that, again, to the leading order, $\mathrm{Nu}_{\mathrm{Q}}^{(1)}$ is independent of β. Given the behavior of $\mathrm{Nu}_{\mathrm{Q}}^{(1)}$ in its asymptotic limits, it is reasonable to approximate Nu_{Q} for small Peclet numbers as a summation of two terms: one that only depends on β and another one that solely changes with Pe.

4.2. Limit of advection-dominated heat transport

Consider the limit of $\mathrm{Pe} \gg 1$, where the thermal boundary layer shrinks at a rate proportional to $\mathrm{Pe}^{-1/3}$. In this case, the temperature and Nusselt number can be described as (see, e.g., [20])

$$T=\mathrm{Pe}^{-1/3}T^{(0)}+\mathrm{Pe}^{-2/3}T^{(1)}+\cdots, \tag{57}$$

$$\mathrm{Nu}_{\mathrm{Q}}=\frac{\mathbb{S}_p}{2\pi\overline{T}^{(0)}}\left(\mathrm{Pe}^{1/3}-\frac{\overline{T}^{(1)}}{\overline{T}^{(0)}}\right)+\cdots. \tag{58}$$

where, upon substituting for T in Eqs. (1) and (3), we have (in generalized boundary layer coordinates)

$$\mathtt{Y}\,\Psi_2\frac{\partial T^{(0)}}{\partial \mathtt{X}}-\frac{\mathtt{Y}^2}{2}\frac{\partial\Psi_2}{\partial \mathtt{X}}\frac{\partial T^{(0)}}{\partial \mathtt{Y}}=\frac{\partial^2 T^{(0)}}{\partial \mathtt{Y}^2}$$

$$\text{with} \quad \frac{\partial T^{(0)}}{\partial \mathtt{Y}}=-1 \quad \text{at} \quad \mathtt{Y}=0 \quad \text{and} \quad \lim_{\mathtt{Y}\to\infty}T^{(0)}=0. \tag{59}$$

Eq. (59) does not depend on β and, in fact, is identical to the one for $\beta=0$. Recognizing that $\overline{T}^{(0)}$ is not a function of β, we deduce from Eq. (58) that Nu_{Q} for large Peclet numbers is approximately equal to the sum of a Pe-dependent term and one that only varies with β.

4.3. Bridging results for limits of low and high Peclet numbers

The main takeaway point of our scaling analyses in Section 4.1 and Section 4.2 is that Nu_{Q} may be estimated as the summation of two terms, one of which is a function of Pe and the other one is a function of β. As a unified formula, we, therefore, propose

$$\mathrm{Nu}_{\mathrm{Q}}\approx\mathrm{Nu}_{\mathrm{Q},0}+\left(\mathrm{Nu}_{\mathrm{Q}}^{c}-\mathrm{Nu}_{\mathrm{Q},0}^{c}\right), \tag{60}$$

where $\mathrm{Nu}_{\mathrm{Q},0}$ represents the value of Nu_{Q} for $\beta=0$ (i.e., for constant conductivity) and the superscript c denotes the Nusselt number corresponding to $\mathrm{Pe}=0$ (i.e, conduction Nusselt number). The above approximation possesses the required form and has zero error for the cases of $\mathrm{Pe}=0$ and $\beta=0$. We will test the validity of Eq. (6) in Section 5.

Before we conclude this section, it is worth emphasizing that, for certain geometries, fairly accurate estimates of $\mathrm{Nu}_{\mathrm{Q},0}$ exist in the literature (see, e.g., [20]). Furthermore, we have discovered empirically that

$$\begin{aligned}\mathrm{Nu}_{\mathrm{Q}}^{c} &= \frac{\mathbb{S}_p\,\beta}{2\pi}\left(\overline{\sqrt{1+2\beta\theta^{(0)}}}-1\right)^{-1}\\ &\approx \frac{\mathbb{S}_p\,\beta}{2\pi}\left(\sqrt{1+2\beta\overline{\theta^{(0)}}}-1\right)^{-1}=\frac{\mathbb{S}_p\,\beta}{2\pi}\left(\sqrt{1+\frac{\mathbb{S}_p\,\beta}{\pi\,\mathrm{Nu}_{\mathrm{Q},0}^{c}}}-1\right)^{-1}.\end{aligned} \tag{61}$$

Eq. (61) is exact for a spherical particle and found to be unexpectedly precise for other particle shapes such as ellipsoids, cylinders, cones, and cubes.

5. Comparison with direct numerical solution of Eq. (1)

In Section 3 and Section 4, we presented approximate formulations for Nu_{T} and Nu_{Q} via perturbation analyses in the asymptotic limits of Pe and β. To give an idea about the estimation error of the proposed formulas, here, we compare their predictions for spherical, cubic, and ellipsoidal particles against the results obtained from the full numerical solution of the problems described in Section 2. A finite-element approach, as implemented in COMSOL Multiphysics [26,27], is employed to carry out the computations. We first solve the steady-state incompressible Navier-Stokes equations for the fluid flow, and, then, use the calculated velocity field $\boldsymbol{u}$ to compute the solution of Eq. (1) for the temperature distribution T. The flow and advection-diffusion equations are solved iteratively, while discretized by P2+P1 and quadratic Lagrange schemes, respectively. The outer boundary at infinity is modeled as a large sphere, whose center coincides with the center of the particle. Specifically, the diameter of the sphere is set to 200 times the characteristic length of the particle. We use tetrahedral elements to mesh the computational domain such that the grid density is the highest near the particle. Grid-independence studies are performed to ensure that the results change only marginally if the mesh is globally refined.

Figs. 1 and 2 show the outcome of our calculations for Nu_{T} and Nu_{Q}, respectively. The results are presented in the form of Δ versus Pe plots for $\beta=0.1,\,1,\,10$ and $\mathrm{Re}=0.1,\,1,\,10,$ where the

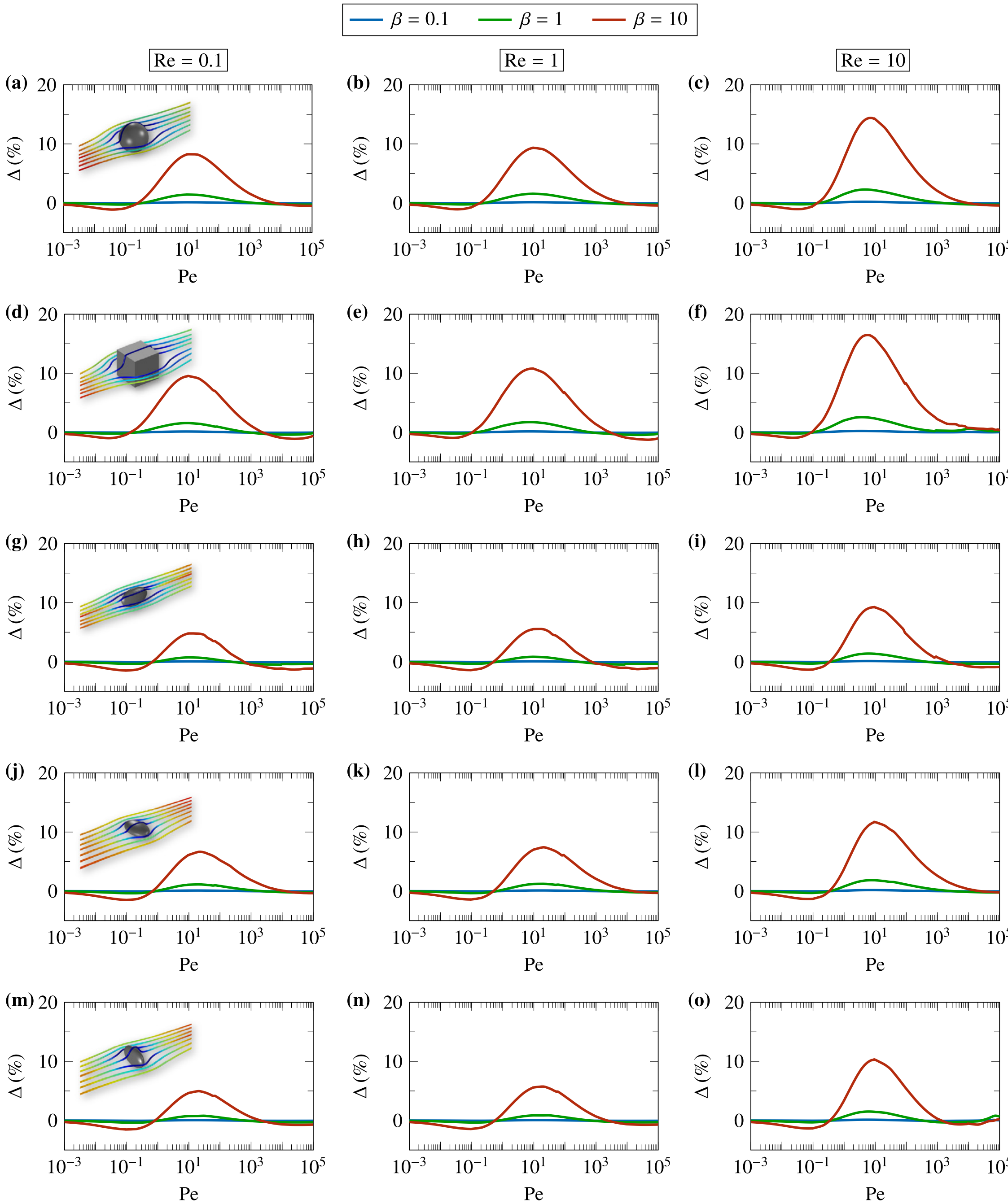

Fig. 1. Percent difference Δ between the results of full numerical simulations and the predictions of Eq. (5) for Nu_T of spherical (first row), cubic (second row), and ellipsoidal (bottom three rows) particles. The plots of Δ versus Pe in the left, middle, and right columns are for $\mathrm{Re} = 0.1$, 1, and 10, respectively. The graphs in the third, fourth, and fifth rows are for flows along the principal axes of the ellipsoid with semi-axis lengths of, respectively, $\mathfrak{a}$, $\mathfrak{b}$, and $\mathfrak{c}$, where $\mathfrak{b}/\mathfrak{a} = 2/3$ and $\mathfrak{c}/\mathfrak{a} = 1/3$. Note that the characteristic length ℓ is set to the radius for the sphere, to half the side length for the cube, and to the largest semi-axis for the ellipsoid.

parameter Δ is defined as the percent difference between the directly computed and predicted values of the Nusselt number. Each figure consists of fifteen sub-figures that are organized into five rows and three columns. The sub-figures in the left, middle, and right columns correspond to $\mathrm{Re} = 0.1$, 1, and 10, respectively. Also, those in the first and second rows belong to spherical and cubic particles, whereas the rest are for an ellipsoidal particle of semi-axis lengths $\mathfrak{a}$, $\mathfrak{b}$, and $\mathfrak{c}$, where $\mathfrak{b}/\mathfrak{a} = 2/3$ and $\mathfrak{c}/\mathfrak{a} = 1/3$. Within the bottom three rows, the plots in the first, second, and third rows are for flows along the principal axes of the ellipsoid associated with $\mathfrak{a}$, $\mathfrak{b}$, and $\mathfrak{c}$, respectively. Note that, in calculating the Nusselt and Peclet numbers the characteristic length ℓ is set to the radius for the sphere, to half the side length for the cube, and to the largest semi-axis for the ellipsoid.

Overall, we see that the predictions of Eqs. (5) and (6) are quite accurate, with the absolute value of Δ being less than 16.5% for all the cases considered. The approximations are more precise for particles with more streamlined shapes. Also, as expected, the estimations deviate the most from the numerical results when β and Re are large and Pe is in the intermediate range. Perhaps surprisingly, however, Δ is very small for $\beta \lesssim O(1)$, irrespective of its corresponding Reynolds and Peclet numbers. Another observation that can be made is that Δ is mostly positive in the plots of Fig. 1 whereas it is mainly negative in those of Fig. 2. Note that

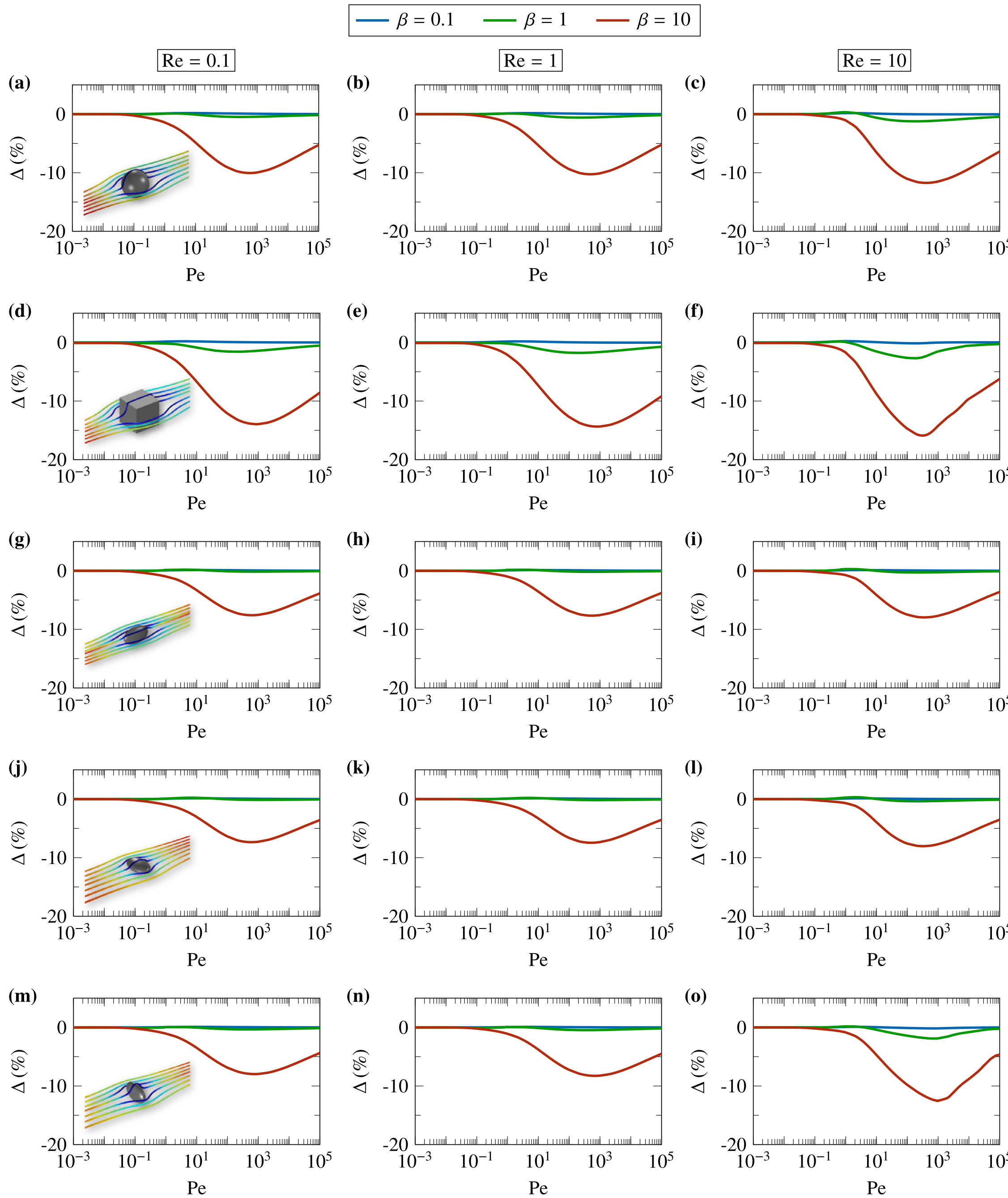

Fig. 2. Percent difference Δ between the results of full numerical simulations and the predictions of Eq. (6) for Nu_Q of spherical (first row), cubic (second row), and ellipsoidal (bottom three rows) particles. The plots of Δ versus Pe in the left, middle, and right columns are for $\mathrm{Re} = 0.1$, 1, and 10, respectively. The graphs in the third, fourth, and fifth rows are for flows along the principal axes of the ellipsoid with semi-axis lengths of, respectively, $\mathfrak{a}$, $\mathfrak{b}$, and $\mathfrak{c}$, where $\mathfrak{b}/\mathfrak{a} = 2/3$ and $\mathfrak{c}/\mathfrak{a} = 1/3$. Note that the characteristic length ℓ is set to the radius for the sphere, to half the side length for the cube, and to the largest semi-axis for the ellipsoid.

Δ is defined such that it is positive when the predicted Nusselt number overestimates the numerically calculated one. Lastly, for the same shape, Re, and β, the Peclet number at which the approximation error is maximum is generally higher for Nu_Q than it is for Nu_T.

6. Summary

We studied the problem of forced convection heat transfer from a particle of arbitrary shape immersed in an unbounded fluid whose thermal conductivity varies linearly with the temperature. Assuming a uniform free-stream flow, we employed asymptotic as well as scaling analyses to develop approximate relations for the variations of the Nusselt number with the Peclet number and the slope of the (normalized) conductivity-temperature curve. We considered both constant temperature and uniform heat flux boundary conditions on the surface of the particle, and discovered that, for the former, Nu_T can be estimated as a product of a Pe-dependent term and one that primarily changes with β. We also found that, for the latter, Nu_Q may be approximated as a sum of a Pe-dependent piece and a β-dependent one. In a nutshell, our derivations offer a straightforward way to estimate the Nusselt number for any β by just knowing the Nusselt number corresponding to $\beta = 0$, i.e., the constant conductivity Nusselt number.

We evaluated the generality and accuracy of our formulations by comparing their predictions for Nu_T and Nu_Q with those calculated based on direct numerical solutions of the governing equations. The comparisons confirmed that the proposed approximations are valid over a wide range of parameters. More specifically, they demonstrated that the estimation errors are remarkably low when $\beta \lesssim O(1)$. Finally, it is worth noting that our formulations are equally applicable for approximating the Sherwood number in equivalent mass transfer problems.

Declaration of Competing Interest

None.

Acknowledgement

Partial support from the National Science Foundation under Grant No. CBET-1749634 is acknowledged. This research was carried out in part using the computational resources provided by the Superior high-performance computing facility at Michigan Technological University.

Appendix A. Derivation of prefactor *c*

We wish to calculate

$$c = -\Gamma\left(\frac{4}{3}\right)(1+\beta)\,\frac{dT^{(0)}}{d\eta}\bigg|_{\eta=0}, \tag{A.1}$$

where $T^{(0)}$ satisfies Eq. (40). We first consider the limit of $\beta \ll 1$ and proceed with a regular perturbation expansion of $T^{(0)}$ as

$$T^{(0)} = T_0^{(0)} + \beta\,T_1^{(0)} + O(\beta^2). \tag{A.2}$$

Substituting Eq. (A.2) in Eq. (40), we find that

$$\frac{d^2T_0^{(0)}}{d\eta^2} + 3\,\eta^2\,\frac{dT_0^{(0)}}{d\eta} = 0 \quad \text{with}$$
$$T_0^{(0)} = 1 \quad \text{at} \quad \eta = 0 \quad \text{and} \quad \lim_{\eta\to\infty} T_0^{(0)} = 0 \tag{A.3}$$

and

$$\frac{d^2T_1^{(0)}}{d\eta^2} + 3\,\eta^2\,\frac{dT_1^{(0)}}{d\eta} + \frac{1}{2}\frac{d^2}{d\eta^2}\left(T_0^{(0)}\right)^2 = 0 \quad \text{with}$$
$$T_1^{(0)} = 0 \quad \text{at} \quad \eta = 0 \quad \text{and} \quad \lim_{\eta\to\infty} T_1^{(0)} = 0. \tag{A.4}$$

The solution of Eq. (A.3) is

$$T_0^{(0)} = 1 - \frac{1}{\Gamma(4/3)}\int_0^{\eta} \exp\left(-\hat{\eta}^3\right)\,d\hat{\eta} \tag{A.5}$$

which is derived using the integrating factor method. Applying the same approach to Eq. (A.4), we obtain (after some mathematical manipulations)

$$\begin{aligned} T_1^{(0)} = {} & \frac{dT_1^{(0)}}{d\eta}\bigg|_{\eta=0}\Gamma(4/3)\left(1-T_0^{(0)}\right) - \frac{\left(1-T_0^{(0)}\right)^2}{2} \\ & - \frac{1}{[\Gamma(4/3)]^2}\int_0^{\eta}\exp\left(-\hat{\eta}^3\right) \\ & \times\left[\Gamma(4/3)\,\hat{\eta}^3 T_0^{(0)} + \int_0^{\hat{\eta}}\hat{\hat{\eta}}^3\exp\left(-\hat{\hat{\eta}}^3\right)d\hat{\hat{\eta}}\right]d\hat{\eta}, \end{aligned} \tag{A.6}$$

where the first term on the right-hand side is numerically calculated (by enforcing the boundary condition at infinity) to be

$$\frac{dT_1^{(0)}}{d\eta}\bigg|_{\eta=0} = 0.667. \tag{A.7}$$

Given Eqs. (A.2), (A.5), and (A.7), for small β, we can write

$$\begin{aligned} c &= 1 + \left[1 - \Gamma\left(\frac{4}{3}\right)\frac{dT_1^{(0)}}{d\eta}\bigg|_{\eta=0}\right]\beta + O(\beta^2) \\ &= 1 + 0.404\,\beta + O(\beta^2). \end{aligned} \tag{A.8}$$

Now, suppose $\beta \gg 1$, while $\beta \ll \mathrm{Pe}$ and $\beta \ll \mathrm{Pr}$. We realize, through inspecting Eq. (40), that $dT^{(0)}/d\eta$ scales with $\beta^{-1/3}$ in this limit. Informed by this scaling, we expand $T^{(0)}$ as

$$T^{(0)} = T_0^{(0)} + O(\beta^{-1/3}) \tag{A.9}$$

and introduce

$$\tilde{\eta} = \beta^{-1/3}\,\eta. \tag{A.10}$$

Replacing for $T^{(0)}$ and η in Eq. (40), we then arrive at

$$\frac{d^2}{d\tilde{\eta}^2}\left[\left(T_0^{(0)}\right)^2\right] + 6\,\tilde{\eta}^2\,\frac{dT_0^{(0)}}{d\tilde{\eta}} = 0 \quad \text{with}$$
$$T_0^{(0)} = 1 \quad \text{at} \quad \tilde{\eta} = 0 \quad \text{and} \quad \lim_{\tilde{\eta}\to\infty} T_1^{(0)} = 0. \tag{A.11}$$

We solve the above nonlinear ordinary differential equation numerically and determine that

$$\begin{aligned} c &= -\Gamma\left(\frac{4}{3}\right)\frac{dT_0^{(0)}}{d\tilde{\eta}}\bigg|_{\tilde{\eta}=0}\beta^{2/3} + O(\beta^{1/3}) \\ &= 0.710\,\beta^{2/3} + O(\beta^{1/3}). \end{aligned} \tag{A.12}$$

What is truly surprising, based on the results of Eqs. (A.8) and (A.12), is that the prefactor c is very well approximated by a single formula (for the entire range of β) as

$$c \approx \left(1 + \frac{3\,\beta}{5}\right)^{2/3}. \tag{A.13}$$

Note that the above expression captures both low- and high-β asymptotes remarkably well.

References

[1] S.K. Das, N. Putra, P. Thiesen, W. Roetzel, Temperature dependence of thermal conductivity enhancement for nanofluids, J. Heat Transf. 125 (4) (2003) 567–574.
[2] W.M. Kays, M.E. Crawford, Convective Heat and Mass Transfer, McGraw-Hill, New York, 1980.
[3] M. Arunachalam, N.R. Rajappa, Forced convection in liquid metals with variable thermal conductivity and capacity, Acta Mech. 31 (1-2) (1978) 25–31.
[4] M. Arunachalam, N.R. Rajappa, Thermal boundary layer in liquid metals with variable thermal conductivity, Flow Turbul. Combust. 34 (2-3) (1978) 179–187.
[5] A.D. Polyanin, Method for solution of some non-linear boundary value problems of a non-stationary diffusion-controlled (thermal) boundary layer, Int. J. Heat Mass Transf. 25 (4) (1982) 471–485.
[6] A.D. Polyanin, An asymptotic analysis of some nonlinear boundary-value problems of convective mass and heat transfer of reacting particles with the flow, Int. J. Heat Mass Transf. 27 (2) (1984) 163–189.
[7] A.D. Polyanin, V.V. Dil'man, The method of asymptotic analogies in the mass and heat transfer theory and chemical engineering science, Int. J. Heat Mass Transf. 33 (6) (1990) 1057–1072.
[8] T.C. Chiam, Heat transfer in a fluid with variable thermal conductivity over a linearly stretching sheet, Acta Mech. 129 (1-2) (1998) 63–72.
[9] W.M. Rohsenow, J.P. Hartnett, Y.I. Cho, Handbook of Heat Transfer, McGraw-Hill New York, New York, 1998.
[10] S. Kakaç, Y. Yener, C.P. Naveira-Cotta, Heat Conduction, CRC Press, Boca Raton, Florida, 2018.
[11] M.A. Ezzat, State space approach to solids and fluids, Can. J. Phys. 86 (11) (2008) 1241–1250.
[12] M.A. Ezzat, A.S. El-Karamany, A.A. El-Bary, On thermo-viscoelasticity with variable thermal conductivity and fractional-order heat transfer, Int. J. Thermophys. 36 (7) (2015) 1684–1697.
[13] M.A. Ezzat, A.A. El-Bary, Effects of variable thermal conductivity and fractional order of heat transfer on a perfect conducting infinitely long hollow cylinder, Int. J. Therm. Sci. 108 (2016) 62–69.
[14] M.A. Ezzat, A.A. El-Bary, Effects of variable thermal conductivity on Stokes' flow of a thermoelectric fluid with fractional order of heat transfer, Int. J. Therm. Sci. 100 (2016) 305–315.

[15] M.A. Ezzat, Fractional thermo-viscoelastic response of biological tissue with variable thermal material properties, J. Therm. Stresses (2020) 1–18.
[16] M.A. Ezzat, The effects of thermal and mechanical material properties on tumorous tissue during hyperthermia treatment, J. Therm. Biol. 92 (2020) 102649.
[17] H. Brenner, Forced convection heat and mass transfer at small Peclet numbers from a particle of arbitrary shape, Chem. Eng. Sci. 18 (2) (1963) 109–122.
[18] A. Acrivos, J.D. Goddard, Asymptotic expansions for laminar forced-convection heat and mass transfer Part 1. Low speed flows, J. Fluid Mech. 23 (2) (1965) 273–291.
[19] L.G. Leal, Advanced Transport Phenomena: Fluid Mechanics and Convective Transport Processes, Cambridge University Press, Cambridge, 2007.
[20] E. Dehdashti, H. Masoud, Forced convection heat transfer from a particle at small and large Peclet numbers, J. Heat Transf. 142 (6) (2020).
[21] V. Vandadi, S.J. Kang, H. Masoud, Reciprocal theorem for convective heat and mass transfer from a particle in Stokes and potential flows, Phys. Rev. Fluids 1 (2) (2016) 022001.
[22] L.M. Relyea, A.S. Khair, Forced convection heat and mass transfer from a slender particle, Chem. Eng. Sci. 174 (2017) 285–289.
[23] H. Masoud, H.A. Stone, The reciprocal theorem in fluid dynamics and transport phenomena, J. Fluid Mech. 879 (2019) P1.
[24] M.J. Lighthill, Contributions to the theory of heat transfer through a laminar boundary layer, Proc. Royal Soc. Lond. 202 (1070) (1950) 359–377.
[25] A. Acrivos, Solution of the laminar boundary layer energy equation at high Prandtl numbers, Phys. Fluids 3 (4) (1960) 657–658.
[26] W.B.J. Zimmerman, Multiphysics Modeling with Finite Element Methods, World Scientific Publishing Company, Singapore, 2006.
[27] D.W. Pepper, J.C. Heinrich, The Finite Element Method: Basic Concepts and Applications with MATLAB, MAPLE, and COMSOL, CRC Press, New York, 2017.